

Supporting Information

Molecular Engineering for Sensitive, Fast and Stable Quasi-Two-Dimensional Perovskite Photodetectors

Wenfeng Li,¹ Qi Wu,¹ Lihua Lu,¹ Yuanyuan Tian,¹ Hongqiang Luo,¹ Yikai Yun,¹ Sijie Jiang,¹

Mengyu Chen,^{*1,2} and Cheng Li^{*1,2}

¹School of Electronic Science and Engineering, Xiamen University, Xiamen 361005, P. R. China

²Future Display Institute of Xiamen, Xiamen 361005, P. R. China

e-mail: mychen@xmu.edu.cn; chengli@xmu.edu.cn;

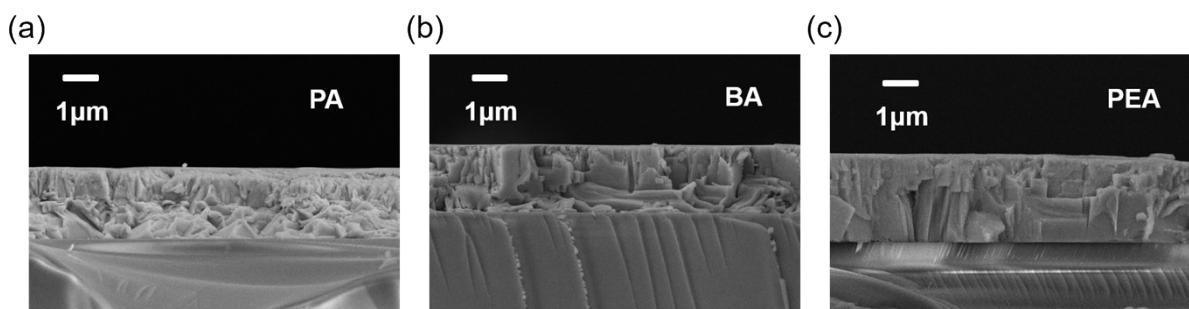


Figure S1. The cross-sectional view of different quasi-2D perovskite films deposited on glass substrate: (a) $(\text{PA})_2(\text{MA})_3\text{Pb}_4\text{I}_{13}$. (b) $(\text{BA})_2(\text{MA})_3\text{Pb}_4\text{I}_{13}$. (c) $(\text{PEA})_2(\text{MA})_3\text{Pb}_4\text{I}_{13}$.

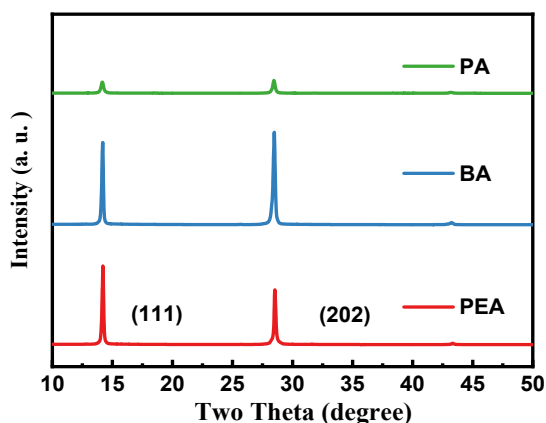


Figure S2. XRD of different quasi-2D perovskite films deposited on glass substrate

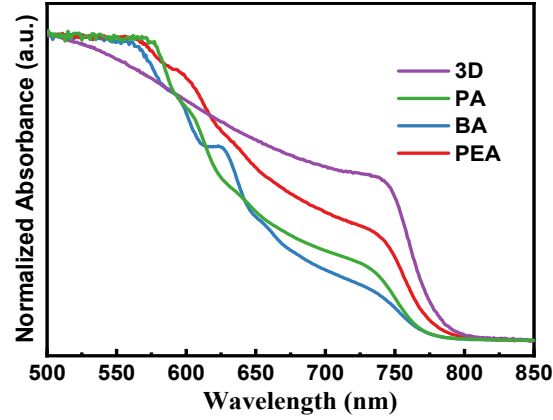


Figure S3. Normalized absorption spectrum comparison of different quasi-2D perovskite and MAPbI₃ films deposited on glass substrate.

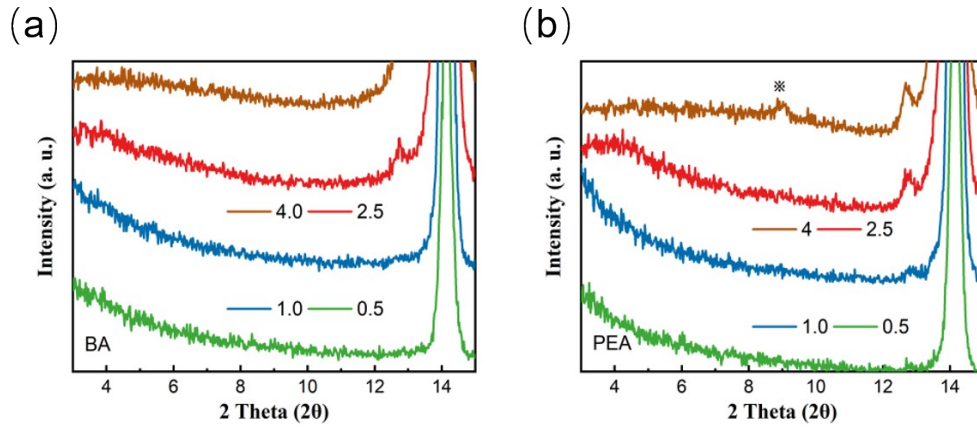


Figure S4 Grazing incidence X-ray diffraction (GiXRD) characterizations with different grazing incidence angles of BA-based (a) and PEA-based (b) quasi-2D perovskite films. 0.5 to 4 are the incident angles.

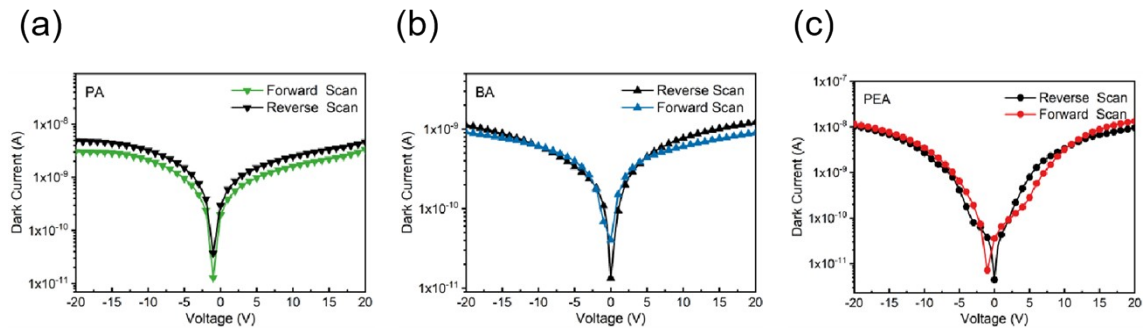


Figure S5 Current-voltage curves of (a) PA- (b) BA- (c) PEA-based quasi-2D perovskite photodetectors under dark with both forward and reverse scanning.

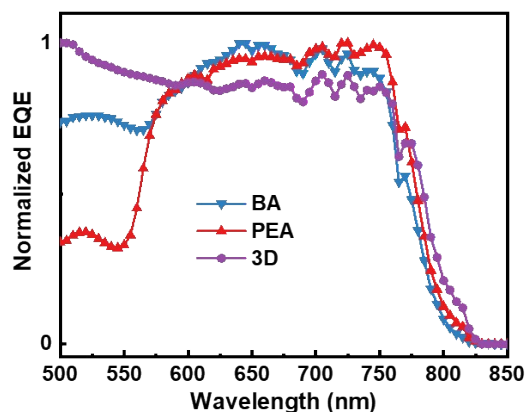


Figure S6. Normalized EQE of different quasi-2D perovskite and MAPbI₃ (3D) based photoconductors.

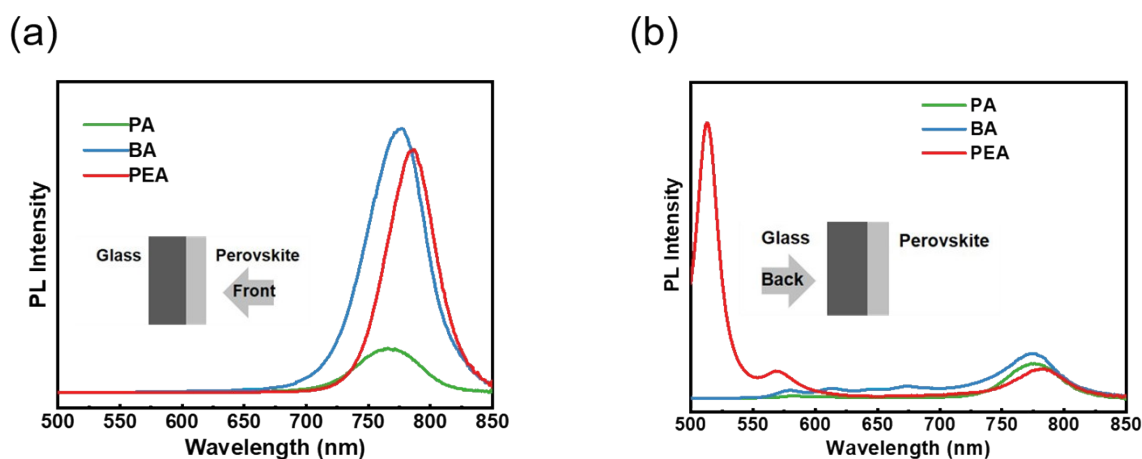


Figure S7. (a-b) Photoluminescence (PL) spectra of perovskite thin films on glass substrates. The perovskite thin films are illuminated from the front (a) and back (b) sides (as illustrated in the insets) under 480nm laser, respectively.

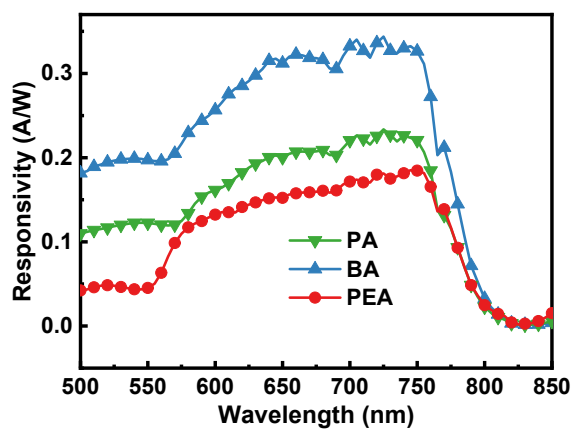


Figure S8. Comparison in responsivity (R) of different quasi-2D perovskite photoconductors.

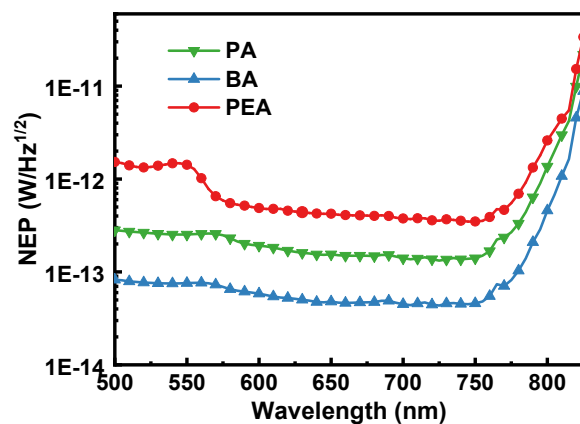


Figure S9. Noise equivalent power (NEP) of different quasi-2D perovskite photoconductors.

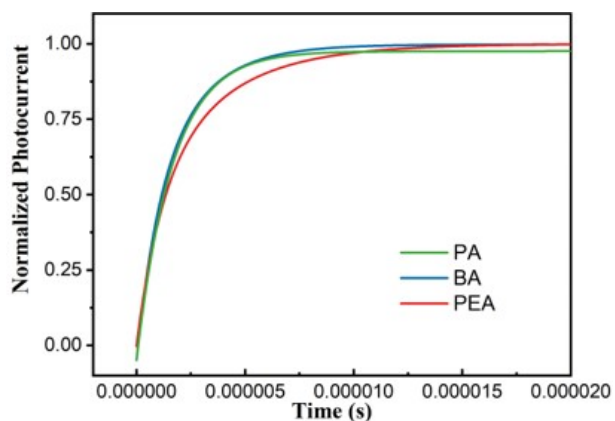


Figure S10. The detail photocurrent rising curves of different quasi-2D perovskite photodetectors to a square-wave modulated light source (525 nm, 1.0 mW/cm² illumination level).

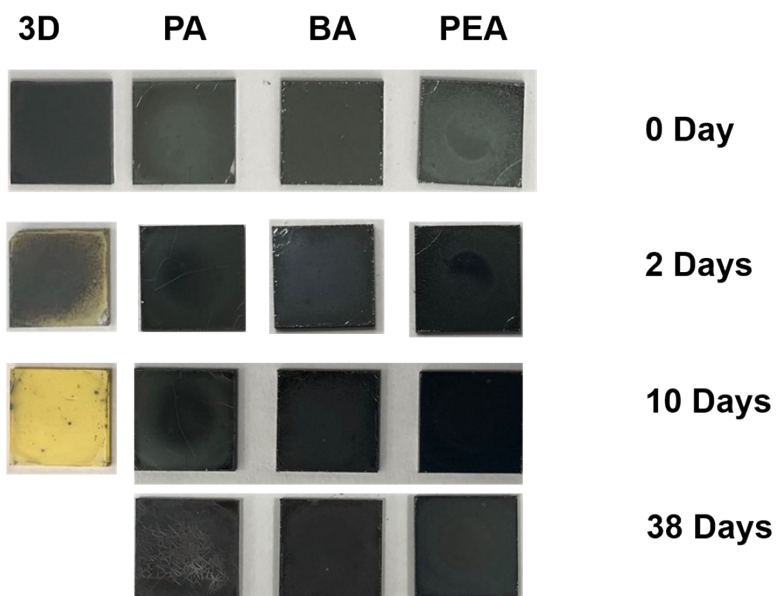


Figure S11. Images of MAPbI₃ and different quasi-2D perovskite films before and after exposure to RH 85%.

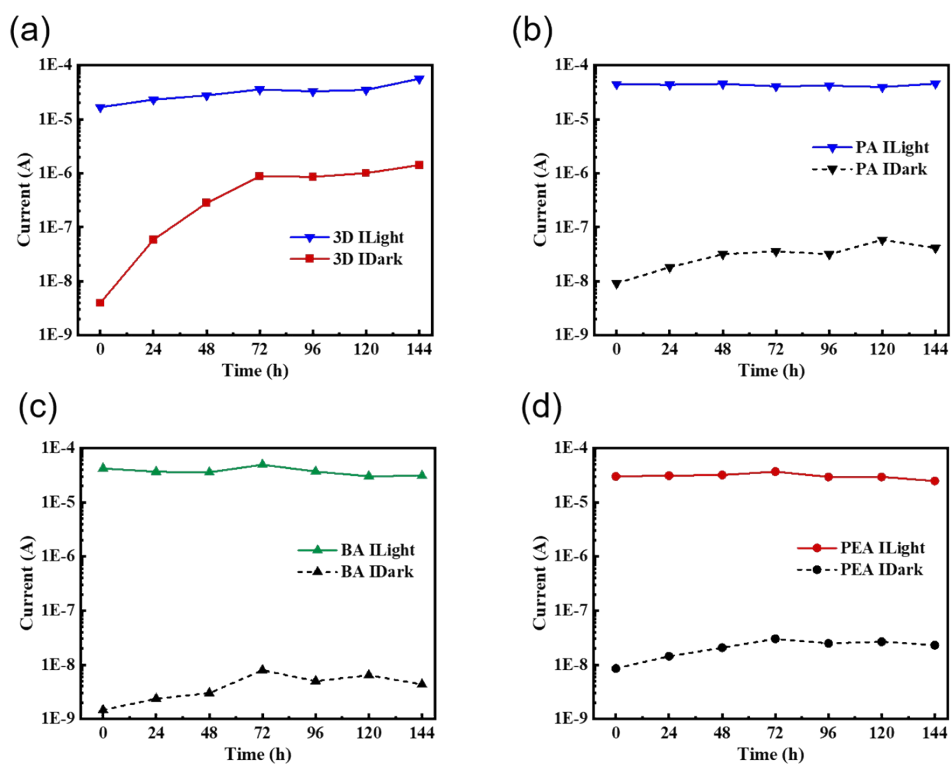


Figure S12. Light and dark currents monitored with ambient exposure time (a) MAPbI₃ (3D); (b) (PA)₂(MA)₃Pb₄I₁₃; (c) (BA)₂(MA)₃Pb₄I₁₃; (d) (PEA)₂(MA)₃Pb₄I₁₃.

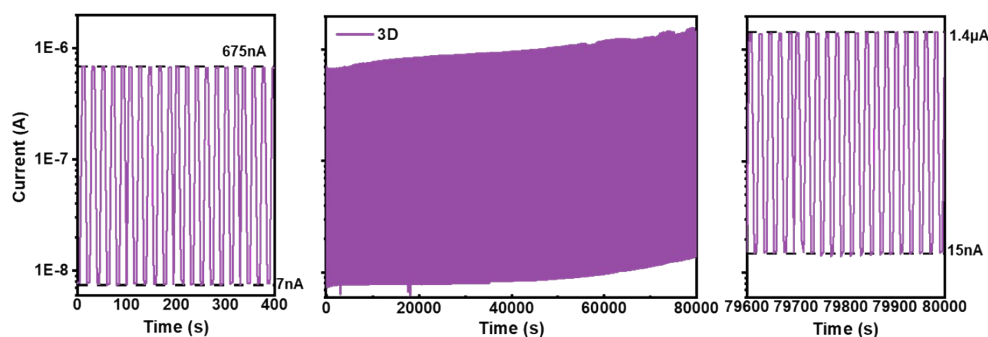


Figure S13. The response of encapsulated MAPbI₃ based photoconductor in a test period of about 80000s ($\lambda=525\text{nm}$, $E_e \approx 1.0\text{mW}/\text{cm}^2$, Bias=5V).

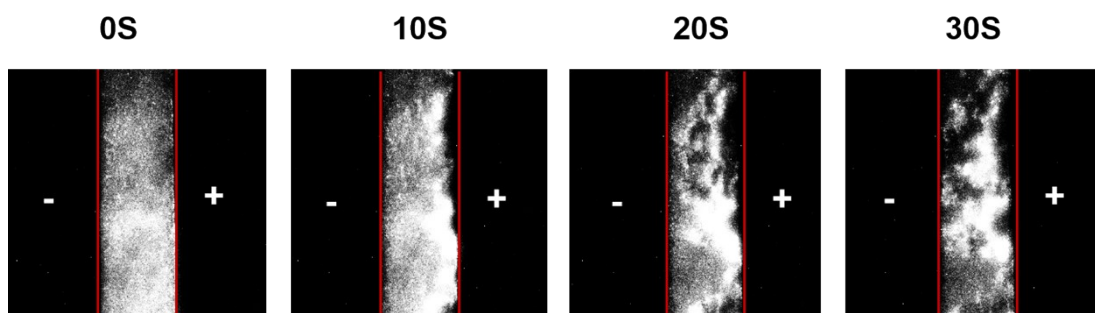


Figure S14. Ion mobility in the perovskite. Time-dependent photoluminescence images at top of (BA)₂(MA)₃Pb₄I₁₃ films deposited on glass under a constant bias (9 V). The symbol "+" represents the positive electrode, and "-" is the negative side. The channel length is 100 μm .

Table S1 The position of photoluminescence (PL) peaks of quasi-2D perovskite thin films fabricated. The perovskite thin films are illuminated from the back sides under 480nm laser.

	3D	PA	BA	PEA	Reference ¹
n=1				513 nm	525 nm
n=2		583nm	580 nm		573 nm
n=3			614 nm		610 nm
n=4			648 nm		
n=other			674 nm		675 nm
n= ∞	781 nm	775nm	775 nm	781 nm	780 nm

Table S2 The Quasi-2D perovskite film thickness measured by step profiler.

Quasi-2D perovskites film	Average thickness (μm)
$(\text{PA})_2(\text{MA})_3\text{Pb}_4\text{I}_{13}$	1.6
$(\text{BA})_2(\text{MA})_3\text{Pb}_4\text{I}_{13}$	1.7
$(\text{PEA})_2(\text{MA})_3\text{Pb}_4\text{I}_{13}$	1.9

Table S3 The rise/fall time of quasi-2D perovskite photodetectors we fabricated.

Device	Rise Time (μs)	Fall Time (μs)
PA-	3.6	39
BA-	3.6	35
PEA-	5.2	95

REFERENCE

1. H. L. Loi, J. P. Cao, X. Y. Guo, C. K. Liu, N. X. Wang, J. J. Song, G. Q. Tang, Y. Zhu and F. Yan, Adv. Sci., 2020, **7**, 2000776.